EVALUATING SOLAR RESOURCE VARIABILITY FROM SATELLITE AND GROUND-BASED OBSERVATIONS

Mary Anderberg, Dave Renné, Thomas Stoffel, and Manajit Sengupta
National Renewable Energy Laboratory
1617 Cole Blvd.
Golden, CO 80401
e-mail: Mary.Anderberg@nrel.gov
David.Renne@nrel.gov
Thomas.Stoffel@nrel.gov
Manajit.Sengupta@nrel.gov

Richard Perez
Atmospheric Sciences Research Center
State University of New York at Albany
251 Fuller Road
Albany, NY 12203
e-mail: perez@asrc.cestm.albany.edu

Paul Stackhouse
National Aeronautics and Space Administration
Langley Research Center
21 Langley Blvd.
Hampton, VA 23681
e-mail: paul.w.stackhouse@nasa.gov

ABSTRACT

This paper examines two co-located satellite-derived data sets over the Atmospheric Radiation Measurement (ARM) Southern Great Plains (SGP) site in central Oklahoma. The data sets, one derived from the National Aeronautics and Space Administration (NASA)/Langley Surface Meteorology and Solar Energy (SSE) Data Base and the other from the State University of New York at Albany (SUNY/Albany) satellite-based model, are compared with each other as well as with a high-quality surface station located at the Central Facility (CF) of the ARM/SGP site. The purpose of the study is two-fold: (1) to benchmark the two satellite-derived data sets with each other and (2) to examine the spatial variability of the higher-resolution SUNY data within the NASA cell that overlays the ground station. The results show variations in seasonal biases between the two satellite-derived data sets and the ground station. In addition, the distribution of high-resolution values within a NASA grid cell varies from month to month possibly due to variations in cloud conditions and surface reflectance characteristics that occur across the seasons.

1. INTRODUCTION

Understanding the local-scale spatial variability of the solar resource has become increasingly important in the past few years for a number of reasons, such as the need for utilities to understand the characteristics of distributed PV systems and their effect on a regional grid. There are also efforts under way to establish global renewable energy data sets so energy analysis modelers can predict future solar deployment levels based on alternative development scenarios. In this case, the modelers rely on global coarse-resolution data sets; however, the values within the individual grid cells, which can be quite large (50–100 km to a side), may not adequately represent the variability of the resource within the cell and therefore may produce serious under- or over-estimates of the resource potential. This study addresses the question of sub-grid solar resource variability within a large (~100 km on a side) grid by examining three concurrent data sets obtained in central Oklahoma: the 100-km-resolution NASA SSE Data Base, which covers the period 1982–2005 (representing the coarse-grid data set); the SUNY/Albany 10-km-resolution 1998–2005 satellite-derived database used in the National Renewable Energy Laboratory's National Solar Radiation Database update (representing the sub-grid-scale data set); and the CF station at the ARM program's SGP research facility located in Central Oklahoma and in operation since around 1991 (to provide ground truth).

To some extent, this research is a continuation of a study originally conducted by Perez, et al (2007) [ref 1], in which sub-grid variability of the NASA SSE cells was studied to determine the degree of consistency in the sub-grid spatial patterns from year to year. However, this study intends to examine more closely the average distribution of variability within NASA SSE coarse-grid cells, and the statistical structure of this variability, to assess to what extent the use of the coarser NASA data may be influenced by the variability within that cell. The study focuses on long-term, concurrent monthly and annual average daily total GHI (global horizontal insolation) data derived from the NASA and SUNY data and the ground-based solar monitoring station at the CF. Although universal conclusions cannot be derived from a single climatic regime such as the SGP, the intent is to provide insights on the uncertainties introduced by using coarse-resolution rather than finer-resolution data for assessment of the solar energy potential.

2. <u>SITE DESCRIPTION</u>

The ARM/SGP site covers a roughly 500-km-by-500-km region over central Kansas and Oklahoma (Fig. 1). The NASA data grids are also shown overlaying the study area. Twenty-three solar monitoring stations—including a major research station, labeled EF-13 and located at the CF—are distributed throughout the area under study. Station EF-13 is located near the exact center of the study area. The analysis in this study focuses on the NASA data cell located EF-13 (Cell #097503650). Within this NASA cell are 100 10-km-resolution cells from the SUNY/Albany model.

The CF is located near Lamont in north-central Oklahoma and is the center of operations for SGP experiments. Three platforms measuring broadband irradiance are co-located within about 25 m (82 ft) of one another at the CF: the Broadband Radiometer Station (BRS), a Solar and Infrared Radiation Station (SIRS), and the SIRS Testbed. Downwelling shortwave irradiance measurements taken by these three radiometer systems are processed to create the Best Estimate Flux (BEFlux) Value Added Product (VAP) described in Long, et al (2002) [ref 2]. Instruments located at the CF receive maintenance daily during the week, and a radiometer calibration facility is located at the CF.

3. <u>DATA SOURCES</u>

3.1 <u>The ARM BEFlux Surface Data</u>

For this study, the ARM/SGP BEFlux data were chosen to represent ground-truth values for the GHI. BEFlux is a VAP created from irradiance measurements available from three co-located surface radiometer platforms at the ARM/SGP CF in Lamont, Oklahoma. The three instrument platforms have the ARM designations SIRS C-01, SIRS EF-13, and BRS. The estimated measurement uncertainty of the BEFlux GHI data is comparable to the pyranometer calibration uncertainties (generally +/-5% for hourly irradiances).

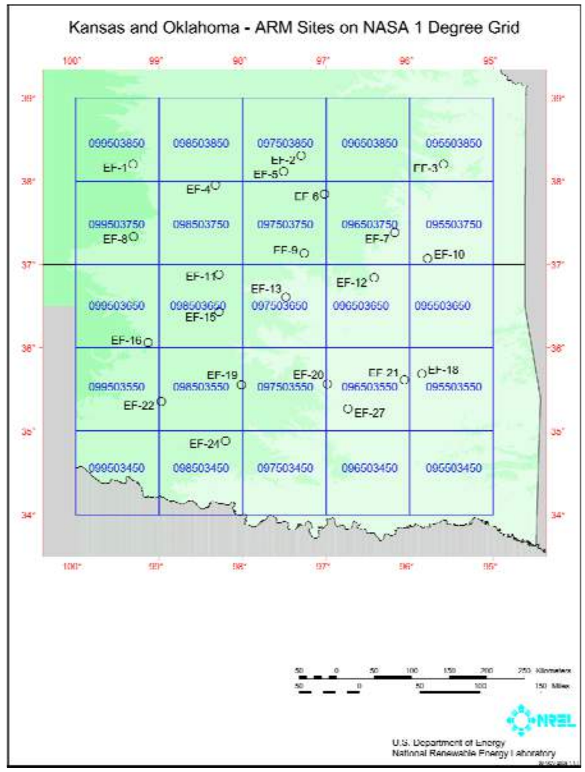

Fig. 1: Location of the ARM/SGP site, including the NASA SSE grid cells overlaying the site and the 23 solar monitoring stations. This study focuses on the cell over the CF (Station EF-13).

The BEFlux data were obtained for this study from the ARM Archive through their online ordering system (http://www.archive.arm.gov/armlogin/login.jsp). The BEFlux data were obtained in netCDF format, and a special utility provided by the ARM program (ARM NetCDF Data eXtract - ANDX) was used to extract the 1-minute GHI data. All ARM data are recorded in Greenwich Mean Time, so they were converted to Central Standard Time. The 1-minute data were then used to calculate hourly averages for all sun-up hours.

3.2 <u>The NASA/SSE Data</u>

Satellite-derived daily total GHI values for this study were obtained from the NASA Langley Atmospheric Science Data Center (ASDC) *Surface Meteorology and Solar Energy Data Set* (http://eosweb.larc.nasa.gov/sse/, ref 3). The data are on a 1º-longitude-by-1º-latitude equal-angle grid covering the entire globe (64,800 regions). The meteorological data are generated using the NASA Goddard

Earth Observing System Version 4 (GEOS 4) Multiyear Assimilation Time Series Data [ref 4]. The GEOS 4 data set has a spacing of 1.25° of longitude by 1° of latitude. Bilinear interpolation is used to produce 1º-by-1º regions.

The solar energy data are generated using an updated version of the Pinker/Laszlo shortwave algorithm [ref. 5]. Cloud data are taken from the International Satellite Cloud Climatology Project DX data set (ISCCP) [ref. 6]. ISCCP DX data are on an equal area grid with an effective 10-by-10-km pixel size subsampled to 30 km. The radiances within a nested grid box containing 44,016 regions. The nested grid has a resolution of 1° latitude globally, and longitudinal resolution ranges from 1° in the tropics and subtropics to 120° at the poles. . Clear and cloudy visible radiances within the grid box are analyzed using empirical relationships between the narrow-band radiances and broadband top-of-atmosphere albedo, a retrieval of the surface albedo, and radiative transfer theory to estimate the downward solar irradiance. The outputs are re-gridded to a 1º equal-angle grid (360 longitudes by 180 latitudes). The re-gridding method is by replication, wherein any grid region that is larger than 1º by 1º is subdivided into 1º-by-1º regions, each with the same value as the original.

3.3 SUNY/Albany 10-km Resolution Data

The SUNY method relies on the visible channel of the Geostationary Environmental Operational Satellite (GOES) located in a stationary orbit directly above the equator [ref. 7]. The method converts successive observations of the reflectance at a given grid cell to estimate a cloud index that is then used in a simple empirical relation to produce an estimate of surface irradiance for that cell. The modeled hourly GHI data produced by the SUNY method were obtained from the SUNY-gridded data, developed as part of the 1991–2005 update of the National Solar Radiation Data Base (NSRDB) [ref. 8]. The data are available on the National Climate Data Center's FTP site (ftp://ftp.ncdc.noaa.gov/pub/data/nsrdb-solar/SUNY-gridded-data/). The SUNY data are on a 0.1º grid; 100 SUNY grid cells are within each NASA/SSE grid cell.

4. DATA PROCESSING

The SUNY hourly GHI values were converted into daily totals for each SUNY cell using all available sun-up data. Sun-up data were defined as data for which the solar zenith angle is less than 90º. The zenith angle is determined at each minute in the hour, so the sun may be up for only part of an hour. The hourly average for such hours, occurring at sunrise and sundown, was determined over the entire hour.

The 1-minute BEFlux data were first adjusted to Central Standard Time, and hourly averages of GHI were calculated for each sun-up hour having at least 5 minutes of available data. Hourly averages were interpolated for those hours having less than 5 minutes of data. Hours missing at sunrise or sunset were extrapolated unless the adjacent sun-up hour was also missing. Daily total GHI was then computed from the hourly average BEFlux. If two or more consecutive hours of data were missing in a day, then the daily total for that day was not calculated.

Monthly, seasonal, and annual average daily totals of GHI for the ARM/SGP BEFlux, for the corresponding 100 SUNY cells, and for the NASA cell (number 097503650 in Fig. 1) were calculated using only the data for those days when BEFlux daily total GHI existed. Running sums of the daily totals were kept for each month (1–13, the thirteenth being the 7-year annual average daily total), season (1–5, the fifth being, again, the 7-year annual average daily total), and year (1998–2005). Also kept were running sums for the number of days of daily totals used in each month, season, and year. The monthly, yearly, and seasonal average daily totals were then determined from the appropriate daily total sum and number of days used for the averaging period.

The SUNY values represent near-instantaneous observations obtained at 15 minutes after the hour (when the GOES scan takes place for that region). These values are then "time-shifted" to produce values at the top of the hour.

5. RESULTS

5.1 Intercomparison of Data Sets

Fig. 2 provides information about the intercomparison of the two satellite-derived data sets with the SGP ground station EF-13. The figure highlights several features.

First, the figure shows that the two satellite-based models tended to underpredict the GHI during the summer and fall and slightly overpredict during the winter. The figure also shows that the variability of the SUNY cells within the NASA grid is generally higher in winter than in summer, most likely because of more complex cloud conditions found in the region during the winter months. Overall, the annual bias (Month 13 in Fig. 2) is slightly negative for both models; that is, the models tend to underpredict actual surface irradiance values relative to the surface measurements.

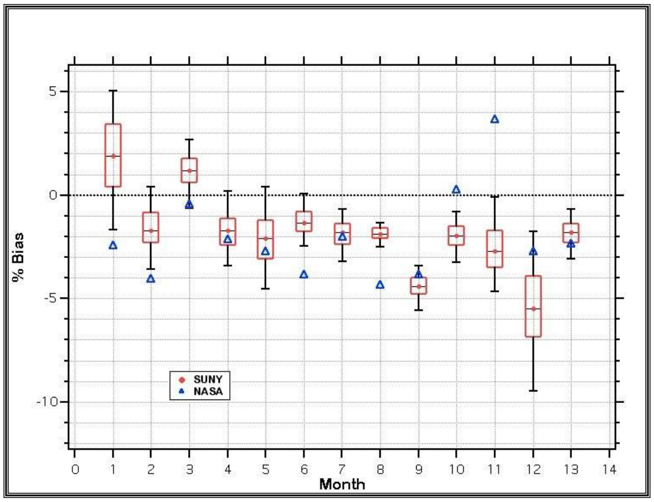

Fig. 2: Percentage bias in the SUNY (red) and NASA (blue) values for monthly average daily total GHI for the period July 1998 to June 2005. The spread shown in the SUNY values represents the standard deviation (red box) and total spread of the 100 values within the NASA grid cell.

5.2 Cell-Specific Intercomparisons

Fig. 3 shows the monthly normalized values of the NASA cell and the specific SUNY cell directly overlaying the SGP EF-13 measurement station. This figure merely confirms what is shown in Fig. 2—that the models tend to underpredict solar resources during the summer months. No explanation has been found for the significant positive bias with the NASA cell during the month of November; this will be investigated further.

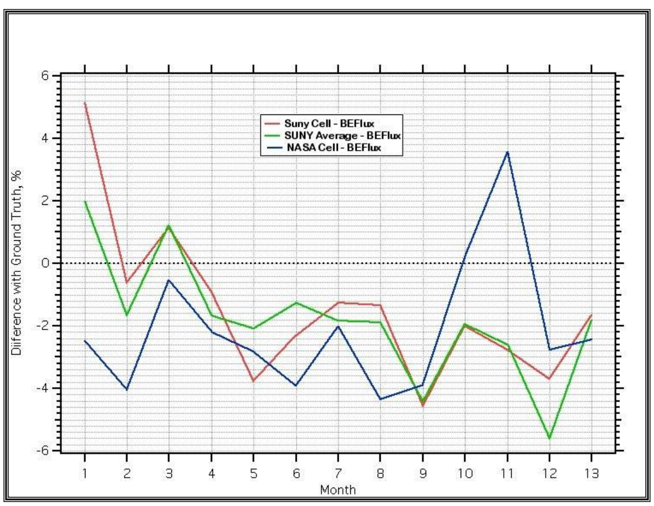

Fig. 3: Percent differences of monthly average daily total GHI: NASA SSE and SUNY cells that coincide with the SGP EF-13 measurement station.

5.3 Distribution of SUNY Data Within the NASA SSE Cell

In this section, we benchmark the SUNY data within a NASA cell to the NASA cell value to examine two issues: the intercomparison of the SUNY model results with the NASA results and the distribution of the SUNY cells within the NASA cell. For example, Fig. 4 shows the distribution of the SUNY values within the NASA cell that overlays the SGP EF-13 measurement station. It is shown that the SUNY and the NASA values in principle are identical for nearly half of all the SUNY values within that cell and that the distribution of the SUNY values is quite narrow. This result indicates that, on an annual basis, the SUNY methodology benchmarks quite well with the NASA methodology.

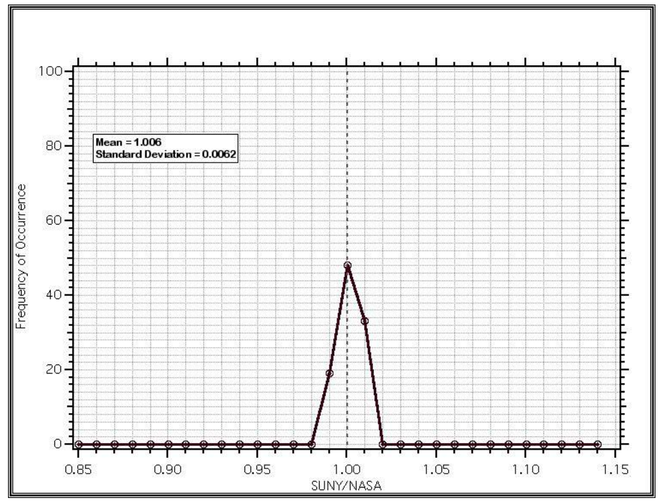

Fig. 4: Annual distribution of the ratio of SUNY/NASA annual mean global irradiance for the 100 SUNY cells within the NASA cell overlaying SGP EF-13 station.

Fig. 5 through Fig. 8 show similar plots for each of the four seasons (winter = December, January, February; spring = March, April, May; summer = June, July, August; fall = September/October/November).

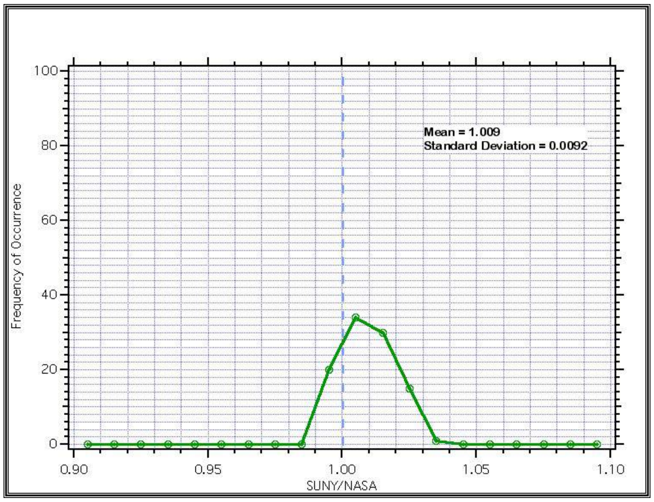

Fig. 5: Same as Fig. 4, spring.

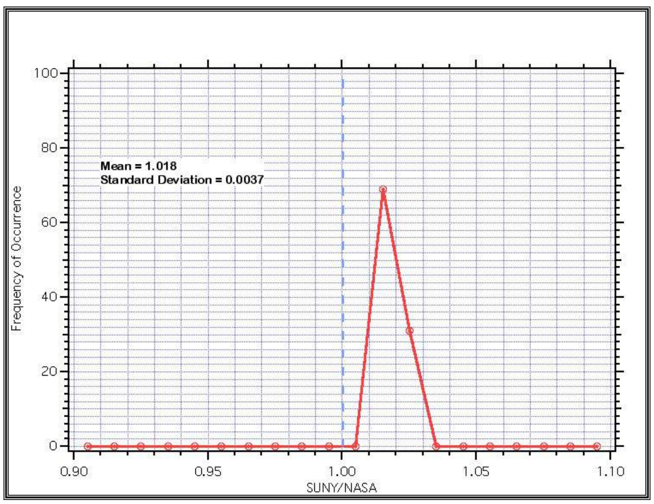

Fig. 6: Same as Fig. 4, summer.

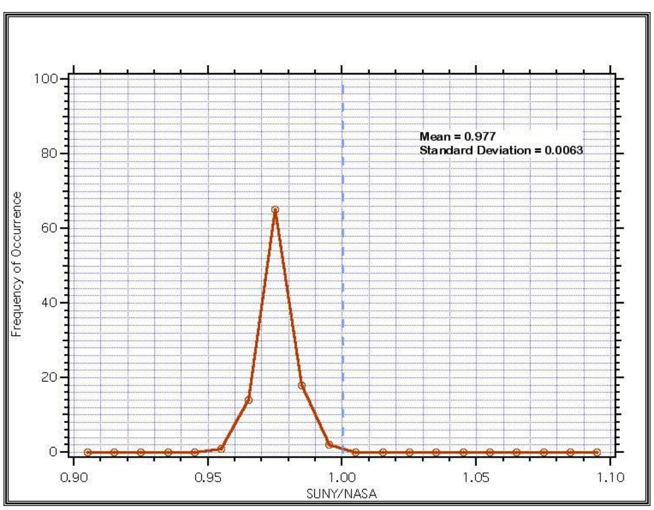

Fig. 7: Same as Fig. 4, fall.

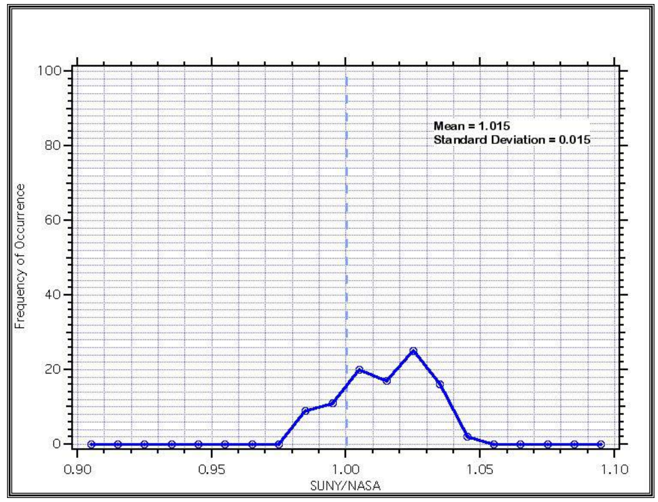

Fig. 8: Same as Fig. 4, winter.

These four figures that, presumably because of changes in cloud characteristics between winter and summer as well as surface albedo or reflectance characteristics, there is much more variability in the microscale solar insolation values during the winter season than in any of the other seasons for this continental mid-latitude climate regime. This characteristic is seen even more clearly by comparing a winter month with a summer month. Fig. 9 and Fig. 10 provide similar plots for December and July, respectively.

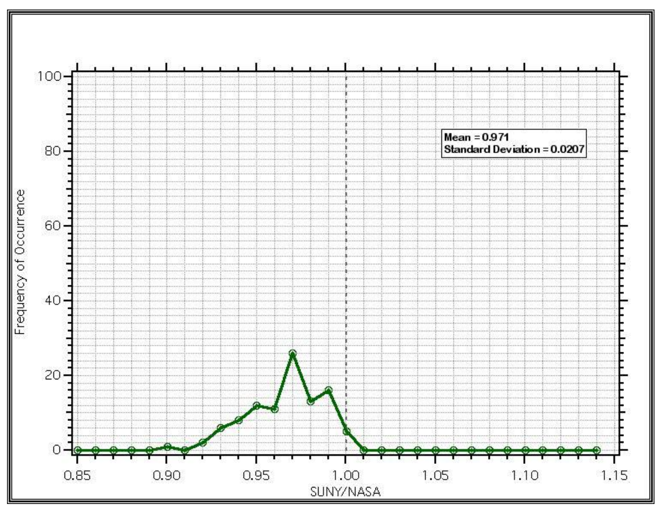

Fig. 9: Same as Fig. 4, December.

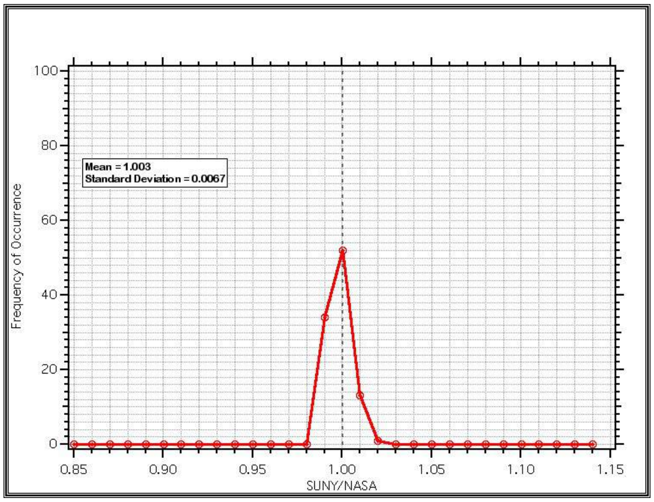

Fig. 10: Same as Fig.4, July.

These figures all indicate that the SUNY values also benchmark more closely with NASA during the spring and summer seasons than during the fall and winter seasons.

6. SUMMARY AND CONCLUSIONS

This study is intended to be the initial step of a longer-term program to understand the influence of sub-grid scale variability on the determination of resource potential and to identify if “upscaling” adjustments would be required when using coarse-grid scale solar resource data. This particular study focused primarily on the benchmarking of two satellite-derived GHI data sets: the coarse-grid (1^0-by-1^0) NASA/SSE and the high-resolution (10-km-by-10-km) SUNY/Albany data set, as well as the intercomparison of these data sets with a high-quality ground station in north-central Oklahoma. This initial study produced several findings:

(1) For the region chosen (a continental mid-latitude Great Plains location) both satellite-derived methods tended to underpredict GHI resources during the summer months and slightly over-predict during the winter, when compared against the ground station.

(2) By benchmarking the two satellite-based methods against each other, it was found that the high-resolution SUNY method tended to produce higher values than the NASA method for all months except during the fall and also came somewhat closer to the ground truth values.

(3) The long-term monthly average mean bias errors for both methods were generally less than $\pm$5%, and for the annual means, the bias errors were approximately -2%.

(4) On an annual basis, the SUNY method compared quite favorably with the NASA method; however, during the fall, the SUNY values were lower than the NASA values, while for the other months, the SUNY values were higher.

(5) The distribution of the 100 SUNY grid cells benchmarked against the NASA cell value was broader during the winter and spring months, which is probably indicative of the more complex cloud conditions and the manner in which the models treat surface reflectance during these periods. Variations in albedo due to agricultural practices across the seasons and around the region may impact the SUNY 10-km x 10-km values in different ways than the NASA 1 x 1 degree value.

In the future, we intend to expand this study to the larger ARM/SGP site to compare the two satellite methods with a more geographically dispersed set of ground observations. We also intend to conduct similar studies in other climatic regimes and for DNI as well as GHI values.

7. ACKNOWLEDGMENTS

This work was supported by the U.S. Department of Energy under Contract No. DE-AC36-08-GO28308 with the National Renewable Energy Laboratory.

8. REFERENCES

(1) Perez, R.; Kmiecik, M.; Stackhouse, P.; Wilcox, S., Enhancing the Geographical and Time Resolution of NASA SSE Time Series Using Microstructuring Patterning, Proceedings Solar 2007, Cleveland, OH, 2007

(2) Long, C.N., The ARM Southern Great Plains Central Facility Best Estimate Radiative Flux CD, Atmospheric Radiation Measurement Program Technical Report, ARM-TR-007, April 2002

(3) Chandler, W. S.; P.W. Stackhouse, Jr.; C.H. Whitlock; J.M. Hoell; D. Westberg; T. Zhang; 2010: Near Real-time Global Radiation and Meteorology Web Services Available from NASA. Proceedings of the Solar 2010 Conference (American Solar Energy Society), May 18-22, Phoenix, Arizona.

(4) Bloom., S. A. da Silva, and D. Dee, 2005; Documentation and Validation of the Goddard Earth Observing System (GEOS) Data Assimilation System – Version 4. NASA Technical Report Series on Global Modeling and Data Assimilation, Max J. Suarez, Editor, NASA/TM-2005-104606, **26**.

(5) Pinker, R. and I. Laszlo, 1992: Modeling of surface solar radiation: Model formulation and validation. *J. Climate Appl. Meteor.*, **24**, 389-401.

(6) Rossow W. B, and R. A. Schiffer, 1999; Advances in understanding clouds from ISCCP, *Bull. Am. Met. Soc.*, 80: 2261-2287.

(7) Perez, R.; P. Ineichen; K. Moore; M. Kmiecik; C. Chain; R. George; F. Vignola, 2002: A New Operational Satellite-to-Irradiance Model – Description and Validation, Solar Energy 73, 5, 307-317

(8) NSRDB, National Solar Radiation Database 1991–2005 Update: User's Manual, NREL/TP-581-41364, April 2007